

EUROPEAN ORGANIZATION FOR NUCLEAR RESEARCH (CERN)



CERN-PH-EP-2012-302

LHCb-PAPER-2012-021

October 15, 2012

Measurement of the CP asymmetry in $B^0 \rightarrow K^{*0} \mu^+ \mu^-$ decays

The LHCb collaboration[†]

Abstract

A measurement of the CP asymmetry in $B^0 \rightarrow K^{*0} \mu^+ \mu^-$ decays is presented, based on 1.0 fb^{-1} of pp collision data recorded by the LHCb experiment during 2011. The measurement is performed in six bins of invariant mass squared of the $\mu^+ \mu^-$ pair, excluding the J/ψ and $\psi(2S)$ resonance regions. Production and detection asymmetries are removed using the $B^0 \rightarrow J/\psi K^{*0}$ decay as a control mode. The integrated CP asymmetry is found to be $-0.072 \pm 0.040 \text{ (stat.)} \pm 0.005 \text{ (syst.)}$, consistent with the Standard Model.

Submitted to Physical Review Letters

[†]Authors are listed on the following pages.

LHCb collaboration

R. Aaij³⁸, C. Abellan Beteta^{33,n}, A. Adametz¹¹, B. Adeua³⁴, M. Adinolfi⁴³, C. Adrover⁶, A. Affolder⁴⁹, Z. Ajaltouni⁵, J. Albrecht³⁵, F. Alessio³⁵, M. Alexander⁴⁸, S. Ali³⁸, G. Alkhazov²⁷, P. Alvarez Cartelle³⁴, A.A. Alves Jr²², S. Amato², Y. Amhis³⁶, L. Anderlini^{17,f}, J. Anderson³⁷, R.B. Appleby⁵¹, O. Aquines Gutierrez¹⁰, F. Archilli^{18,35}, A. Artamonov³², M. Artuso⁵³, E. Aslanides⁶, G. Auriemma^{22,m}, S. Bachmann¹¹, J.J. Back⁴⁵, C. Baesso⁵⁴, V. Balagura^{36,28}, W. Baldini¹⁶, R.J. Barlow⁵¹, C. Barschel³⁵, S. Barsuk⁷, W. Barter⁴⁴, A. Bates⁴⁸, Th. Bauer³⁸, A. Bay³⁶, J. Beddow⁴⁸, I. Bediaga¹, S. Belogurov²⁸, K. Belous³², I. Belyaev²⁸, E. Ben-Haim⁸, M. Benayoun⁸, G. Bencivenni¹⁸, S. Benson⁴⁷, J. Benton⁴³, A. Berezhnoy²⁹, R. Bernet³⁷, M.-O. Bettler⁴⁴, M. van Beuzekom³⁸, A. Bien¹¹, S. Bifani¹², T. Bird⁵¹, A. Bizzeti^{17,h}, P.M. Bjørnstad⁵¹, T. Blake³⁵, F. Blanc³⁶, C. Blanks⁵⁰, J. Blouw¹¹, S. Blusk⁵³, A. Bobrov³¹, V. Bocci²², A. Bondar³¹, N. Bondar²⁷, W. Bonivento¹⁵, S. Borghi^{48,51}, A. Borgia⁵³, T.J.V. Bowcock⁴⁹, C. Bozzi¹⁶, T. Brambach⁹, J. van den Brand³⁹, J. Bressieux³⁶, D. Brett⁵¹, M. Britsch¹⁰, T. Britton⁵³, N.H. Brook⁴³, H. Brown⁴⁹, A. Büchlér-Germann³⁷, I. Burducea²⁶, A. Bursche³⁷, J. Buytaert³⁵, S. Cadeddu¹⁵, O. Callot⁷, M. Calvi^{20,j}, M. Calvo Gomez^{33,n}, A. Camboni³³, P. Campana^{18,35}, A. Carbone^{14,c}, G. Carboni^{21,k}, R. Cardinale^{19,i}, A. Cardini¹⁵, L. Carson⁵⁰, K. Carvalho Akiba², G. Casse⁴⁹, M. Cattaneo³⁵, Ch. Cauet⁹, M. Charles⁵², Ph. Charpentier³⁵, P. Chen^{3,36}, N. Chiapolini³⁷, M. Chrzaszcz²³, K. Ciba³⁵, X. Cid Vidal³⁴, G. Ciezarek⁵⁰, P.E.L. Clarke⁴⁷, M. Clemencic³⁵, H.V. Cliff⁴⁴, J. Closier³⁵, C. Coca²⁶, V. Coco³⁸, J. Cogan⁶, E. Cogneras⁵, P. Collins³⁵, A. Comerma-Montells³³, A. Contu^{52,15}, A. Cook⁴³, M. Coombes⁴³, G. Corti³⁵, B. Couturier³⁵, G.A. Cowan³⁶, D. Craik⁴⁵, S. Cunliffe⁵⁰, R. Currie⁴⁷, C. D'Ambrosio³⁵, P. David⁸, P.N.Y. David³⁸, I. De Bonis⁴, K. De Bruyn³⁸, S. De Capua^{21,k}, M. De Cian³⁷, J.M. De Miranda¹, L. De Paula², P. De Simone¹⁸, D. Decamp⁴, M. Deckenhoff⁹, H. Degaudenzi^{36,35}, L. Del Buono⁸, C. Deplano¹⁵, D. Derkach¹⁴, O. Deschamps⁵, F. Dettori³⁹, J. Dickens⁴⁴, H. Dijkstra³⁵, P. Diniz Batista¹, F. Domingo Bonal^{33,n}, S. Donleavy⁴⁹, F. Dordei¹¹, A. Dosil Suárez³⁴, D. Dossett⁴⁵, A. Dovbnya⁴⁰, F. Dupertuis³⁶, R. Dzhelyadin³², A. Dziurda²³, A. Dzyuba²⁷, S. Easo⁴⁶, U. Egede⁵⁰, V. Egorychev²⁸, S. Eidelman³¹, D. van Eijk³⁸, F. Eisele¹¹, S. Eisenhardt⁴⁷, R. Ekelhof⁹, L. Eklund⁴⁸, I. El Rifai⁵, Ch. Elsasser³⁷, D. Elsby⁴², D. Esperante Pereira³⁴, A. Falabella^{14,e}, C. Färber¹¹, G. Fardell⁴⁷, C. Farinelli³⁸, S. Farry¹², V. Fave³⁶, V. Fernandez Albor³⁴, F. Ferreira Rodrigues¹, M. Ferro-Luzzi³⁵, S. Filippov³⁰, C. Fitzpatrick³⁵, M. Fontana¹⁰, F. Fontanelli^{19,i}, R. Forty³⁵, O. Francisco², M. Frank³⁵, C. Frei³⁵, M. Frosini^{17,f}, S. Furcas²⁰, A. Gallas Torreira³⁴, D. Galli^{14,c}, M. Gandelman², P. Gandini⁵², Y. Gao³, J.-C. Garnier³⁵, J. Garofoli⁵³, J. Garra Tico⁴⁴, L. Garrido³³, C. Gaspar³⁵, R. Gauld⁵², E. Gersabeck¹¹, M. Gersabeck³⁵, T. Gershon^{45,35}, Ph. Ghez⁴, V. Gibson⁴⁴, V.V. Gligorov³⁵, C. Göbel⁵⁴, D. Golubkov²⁸, A. Golutvin^{50,28,35}, A. Gomes², H. Gordon⁵², M. Grabalosa Gándara³³, R. Graciani Diaz³³, L.A. Granado Cardoso³⁵, E. Graugés³³, G. Graziani¹⁷, A. Grecu²⁶, E. Greening⁵², S. Gregson⁴⁴, O. Grünberg⁵⁵, B. Gui⁵³, E. Gushchin³⁰, Yu. Guz³², T. Gys³⁵, C. Hadjivasilou⁵³, G. Haefeli³⁶, C. Haen³⁵, S.C. Haines⁴⁴, S. Hall⁵⁰, T. Hampson⁴³, S. Hansmann-Menzemer¹¹, N. Harnew⁵², S.T. Harnew⁴³, J. Harrison⁵¹, P.F. Harrison⁴⁵, T. Hartmann⁵⁵, J. He⁷, V. Heijne³⁸, K. Hennessy⁴⁹, P. Henrard⁵, J.A. Hernando Morata³⁴, E. van Herwijnen³⁵, E. Hicks⁴⁹, D. Hill⁵², M. Hoballah⁵, P. Hopchev⁴, W. Hulsbergen³⁸, P. Hunt⁵², T. Huse⁴⁹, N. Hussain⁵², R.S. Huston¹², D. Hutchcroft⁴⁹, D. Hynds⁴⁸, V. Iakovenko⁴¹, P. Ilten¹², J. Imong⁴³, R. Jacobsson³⁵, A. Jaeger¹¹, M. Jahjah Hussein⁵,

E. Jans³⁸, F. Jansen³⁸, P. Jaton³⁶, B. Jean-Marie⁷, F. Jing³, M. John⁵², D. Johnson⁵²,
 C.R. Jones⁴⁴, B. Jost³⁵, M. Kaballo⁹, S. Kandybei⁴⁰, M. Karacson³⁵, M. Karbach³⁵,
 J. Keaveney¹², I.R. Kenyon⁴², U. Kerzel³⁵, T. Ketel³⁹, A. Keune³⁶, B. Khanji²⁰, Y.M. Kim⁴⁷,
 O. Kochebina⁷, I. Komarov²⁹, V. Komarov³⁶, R.F. Koopman³⁹, P. Koppenburg³⁸,
 M. Korolev²⁹, A. Kozlinskiy³⁸, L. Kravchuk³⁰, K. Kreplin¹¹, M. Kreps⁴⁵, G. Krocker¹¹,
 P. Krokovny³¹, F. Kruse⁹, M. Kucharczyk^{20,23,j}, V. Kudryavtsev³¹, T. Kvaratskheliya^{28,35},
 V.N. La Thi³⁶, D. Lacarrere³⁵, G. Lafferty⁵¹, A. Lai¹⁵, D. Lambert⁴⁷, R.W. Lambert³⁹,
 E. Lanciotti³⁵, G. Lanfranchi^{18,35}, C. Langenbruch³⁵, T. Latham⁴⁵, C. Lazzeroni⁴²,
 R. Le Gac⁶, J. van Leerdam³⁸, J.-P. Lees⁴, R. Lefèvre⁵, A. Leflat^{29,35}, J. Lefrançois⁷,
 O. Leroy⁶, T. Lesiak²³, L. Li³, Y. Li³, L. Li Gioi⁵, M. Liles⁴⁹, R. Lindner³⁵, C. Linn¹¹, B. Liu³,
 G. Liu³⁵, J. von Loeben²⁰, J.H. Lopes², E. Lopez Asamar³³, N. Lopez-March³⁶, H. Lu³,
 J. Luisier³⁶, A. Mac Raighne⁴⁸, F. Machefert⁷, I.V. Machikhiliyan^{4,28}, F. Maciuc²⁶,
 O. Maev^{27,35}, J. Magnin¹, M. Maino²⁰, S. Malde⁵², G. Manca^{15,d}, G. Mancinelli⁶,
 N. Mangiafave⁴⁴, U. Marconi¹⁴, R. Märki³⁶, J. Marks¹¹, G. Martellotti²², A. Martens⁸,
 L. Martin⁵², A. Martín Sánchez⁷, M. Martinelli³⁸, D. Martinez Santos³⁵, A. Massafferri¹,
 Z. Mathe³⁵, C. Matteuzzi²⁰, M. Matveev²⁷, E. Maurice⁶, A. Mazurov^{16,30,35}, J. McCarthy⁴²,
 G. McGregor⁵¹, R. McNulty¹², M. Meissner¹¹, M. Merk³⁸, J. Merkel⁹, D.A. Milanes¹³,
 M.-N. Minard⁴, J. Molina Rodriguez⁵⁴, S. Monteil⁵, D. Moran⁵¹, P. Morawski²³,
 R. Mountain⁵³, I. Mous³⁸, F. Muheim⁴⁷, K. Müller³⁷, R. Muresan²⁶, B. Muryn²⁴, B. Muster³⁶,
 J. Mylroie-Smith⁴⁹, P. Naik⁴³, T. Nakada³⁶, R. Nandakumar⁴⁶, I. Nasteva¹, M. Needham⁴⁷,
 N. Neufeld³⁵, A.D. Nguyen³⁶, C. Nguyen-Mau^{36,o}, M. Nicol⁷, V. Niess⁵, N. Nikitin²⁹,
 T. Nikodem¹¹, A. Nomerotski^{52,35}, A. Novoselov³², A. Oblakowska-Mucha²⁴, V. Obraztsov³²,
 S. Oggero³⁸, S. Ogilvy⁴⁸, O. Okhrimenko⁴¹, R. Oldeman^{15,d,35}, M. Orlandea²⁶,
 J.M. Otalora Goicochea², P. Owen⁵⁰, B.K. Pal⁵³, A. Palano^{13,b}, M. Palutan¹⁸, J. Panman³⁵,
 A. Papanestis⁴⁶, M. Pappagallo⁴⁸, C. Parkes⁵¹, C.J. Parkinson⁵⁰, G. Passaleva¹⁷, G.D. Patel⁴⁹,
 M. Patel⁵⁰, G.N. Patrick⁴⁶, C. Patrignani^{19,i}, C. Pavel-Nicorescu²⁶, A. Pazos Alvarez³⁴,
 A. Pellegrino³⁸, G. Penso^{22,l}, M. Pepe Altarelli³⁵, S. Perazzini^{14,c}, D.L. Perego^{20,j},
 E. Perez Trigo³⁴, A. Pérez-Calero Yzquierdo³³, P. Perret⁵, M. Perrin-Terrin⁶, G. Pessina²⁰,
 K. Petridis⁵⁰, A. Petrolini^{19,i}, A. Phan⁵³, E. Picatoste Olloqui³³, B. Pie Valls³³, B. Pietrzyk⁴,
 T. Pilar⁴⁵, D. Pinci²², S. Playfer⁴⁷, M. Plo Casasus³⁴, F. Polci⁸, G. Polok²³, A. Poluektov^{45,31},
 E. Polycarpo², D. Popov¹⁰, B. Popovici²⁶, C. Potterat³³, A. Powell⁵², J. Prisciandaro³⁶,
 V. Pugatch⁴¹, A. Puig Navarro³⁶, W. Qian³, J.H. Rademacker⁴³, B. Rakotomiaramanana³⁶,
 M.S. Rangel², I. Raniuk⁴⁰, N. Rauschmayr³⁵, G. Raven³⁹, S. Redford⁵², M.M. Reid⁴⁵,
 A.C. dos Reis¹, S. Ricciardi⁴⁶, A. Richards⁵⁰, K. Rinnert⁴⁹, V. Rives Molina³³,
 D.A. Roa Romero⁵, P. Robbe⁷, E. Rodrigues^{48,51}, P. Rodriguez Perez³⁴, G.J. Rogers⁴⁴,
 S. Roiser³⁵, V. Romanovsky³², A. Romero Vidal³⁴, J. Rouvinet³⁶, T. Ruf³⁵, H. Ruiz³³,
 G. Sabatino^{21,k}, J.J. Saborido Silva³⁴, N. Sagidova²⁷, P. Sail⁴⁸, B. Saitta^{15,d}, C. Salzmann³⁷,
 B. Sanmartin Sedes³⁴, M. Sannino^{19,i}, R. Santacesaria²², C. Santamarina Rios³⁴,
 R. Santinelli³⁵, E. Santovetti^{21,k}, M. Sapunov⁶, A. Sarti^{18,l}, C. Satriano^{22,m}, A. Satta²¹,
 M. Savrie^{16,e}, D. Savrina²⁸, P. Schaack⁵⁰, M. Schiller³⁹, H. Schindler³⁵, S. Schleich⁹,
 M. Schlupp⁹, M. Schmelling¹⁰, B. Schmidt³⁵, O. Schneider³⁶, A. Schopper³⁵, M.-H. Schune⁷,
 R. Schwemmer³⁵, B. Sciascia¹⁸, A. Sciubba^{18,l}, M. Seco³⁴, A. Semennikov²⁸, K. Senderowska²⁴,
 I. Sepp⁵⁰, N. Serra³⁷, J. Serrano⁶, P. Seyfert¹¹, M. Shapkin³², I. Shapoval^{40,35}, P. Shatalov²⁸,
 Y. Shcheglov²⁷, T. Shears^{49,35}, L. Shekhtman³¹, O. Shevchenko⁴⁰, V. Shevchenko²⁸,
 A. Shires⁵⁰, R. Silva Coutinho⁴⁵, T. Skwarnicki⁵³, N.A. Smith⁴⁹, E. Smith^{52,46}, M. Smith⁵¹,
 K. Sobczak⁵, F.J.P. Soler⁴⁸, A. Solomin⁴³, F. Soomro^{18,35}, D. Souza De Paula²,

B. Spaan⁹, A. Sparkes⁴⁷, P. Spradlin⁴⁸, F. Stagni³⁵, S. Stahl¹¹, O. Steinkamp³⁷, S. Stoica²⁶, S. Stone⁵³, B. Storaci³⁸, M. Straticiuc²⁶, U. Straumann³⁷, V.K. Subbiah³⁵, S. Swientek⁹, M. Szczekowski²⁵, P. Szczypka^{36,35}, T. Szumlak²⁴, S. T'Jampens⁴, M. Teklishyn⁷, E. Teodorescu²⁶, F. Teubert³⁵, C. Thomas⁵², E. Thomas³⁵, J. van Tilburg¹¹, V. Tisserand⁴, M. Tobin³⁷, S. Tolk³⁹, S. Topp-Joergensen⁵², N. Torr⁵², E. Tournefier^{4,50}, S. Tourneur³⁶, M.T. Tran³⁶, A. Tsaregorodtsev⁶, N. Tuning³⁸, M. Ubeda Garcia³⁵, A. Ukleja²⁵, D. Urner⁵¹, U. Uwer¹¹, V. Vagnoni¹⁴, G. Valenti¹⁴, R. Vazquez Gomez³³, P. Vazquez Regueiro³⁴, S. Vecchi¹⁶, J.J. Velthuis⁴³, M. Veltri^{17,g}, G. Veneziano³⁶, M. Vesterinen³⁵, B. Viaud⁷, I. Videau⁷, D. Vieira², X. Vilasis-Cardona^{33,n}, J. Visniakov³⁴, A. Vollhardt³⁷, D. Volyanskyy¹⁰, D. Voong⁴³, A. Vorobyev²⁷, V. Vorobyev³¹, H. Voss¹⁰, C. Voß⁵⁵, R. Waldi⁵⁵, R. Wallace¹², S. Wandernoth¹¹, J. Wang⁵³, D.R. Ward⁴⁴, N.K. Watson⁴², A.D. Webber⁵¹, D. Websdale⁵⁰, M. Whitehead⁴⁵, J. Wicht³⁵, D. Wiedner¹¹, L. Wiggers³⁸, G. Wilkinson⁵², M.P. Williams^{45,46}, M. Williams^{50,p}, F.F. Wilson⁴⁶, J. Wishahi⁹, M. Witek^{23,35}, W. Witzeling³⁵, S.A. Wotton⁴⁴, S. Wright⁴⁴, S. Wu³, K. Wyllie³⁵, Y. Xie⁴⁷, F. Xing⁵², Z. Xing⁵³, Z. Yang³, R. Young⁴⁷, X. Yuan³, O. Yushchenko³², M. Zangoli¹⁴, M. Zavertyaev^{10,a}, F. Zhang³, L. Zhang⁵³, W.C. Zhang¹², Y. Zhang³, A. Zhelezov¹¹, L. Zhong³, A. Zvyagin³⁵.

¹Centro Brasileiro de Pesquisas Físicas (CBPF), Rio de Janeiro, Brazil

²Universidade Federal do Rio de Janeiro (UFRJ), Rio de Janeiro, Brazil

³Center for High Energy Physics, Tsinghua University, Beijing, China

⁴LAPP, Université de Savoie, CNRS/IN2P3, Annecy-Le-Vieux, France

⁵Clermont Université, Université Blaise Pascal, CNRS/IN2P3, LPC, Clermont-Ferrand, France

⁶CPPM, Aix-Marseille Université, CNRS/IN2P3, Marseille, France

⁷LAL, Université Paris-Sud, CNRS/IN2P3, Orsay, France

⁸LPNHE, Université Pierre et Marie Curie, Université Paris Diderot, CNRS/IN2P3, Paris, France

⁹Fakultät Physik, Technische Universität Dortmund, Dortmund, Germany

¹⁰Max-Planck-Institut für Kernphysik (MPIK), Heidelberg, Germany

¹¹Physikalisches Institut, Ruprecht-Karls-Universität Heidelberg, Heidelberg, Germany

¹²School of Physics, University College Dublin, Dublin, Ireland

¹³Sezione INFN di Bari, Bari, Italy

¹⁴Sezione INFN di Bologna, Bologna, Italy

¹⁵Sezione INFN di Cagliari, Cagliari, Italy

¹⁶Sezione INFN di Ferrara, Ferrara, Italy

¹⁷Sezione INFN di Firenze, Firenze, Italy

¹⁸Laboratori Nazionali dell'INFN di Frascati, Frascati, Italy

¹⁹Sezione INFN di Genova, Genova, Italy

²⁰Sezione INFN di Milano Bicocca, Milano, Italy

²¹Sezione INFN di Roma Tor Vergata, Roma, Italy

²²Sezione INFN di Roma La Sapienza, Roma, Italy

²³Henryk Niewodniczanski Institute of Nuclear Physics Polish Academy of Sciences, Kraków, Poland

²⁴AGH University of Science and Technology, Kraków, Poland

²⁵National Center for Nuclear Research (NCBJ), Warsaw, Poland

²⁶Horia Hulubei National Institute of Physics and Nuclear Engineering, Bucharest-Magurele, Romania

²⁷Petersburg Nuclear Physics Institute (PNPI), Gatchina, Russia

²⁸Institute of Theoretical and Experimental Physics (ITEP), Moscow, Russia

²⁹Institute of Nuclear Physics, Moscow State University (SINP MSU), Moscow, Russia

³⁰Institute for Nuclear Research of the Russian Academy of Sciences (INR RAN), Moscow, Russia

³¹Budker Institute of Nuclear Physics (SB RAS) and Novosibirsk State University, Novosibirsk, Russia

³²Institute for High Energy Physics (IHEP), Protvino, Russia

³³Universitat de Barcelona, Barcelona, Spain

- ³⁴Universidad de Santiago de Compostela, Santiago de Compostela, Spain
³⁵European Organization for Nuclear Research (CERN), Geneva, Switzerland
³⁶Ecole Polytechnique Fédérale de Lausanne (EPFL), Lausanne, Switzerland
³⁷Physik-Institut, Universität Zürich, Zürich, Switzerland
³⁸Nikhef National Institute for Subatomic Physics, Amsterdam, The Netherlands
³⁹Nikhef National Institute for Subatomic Physics and VU University Amsterdam, Amsterdam, The Netherlands
⁴⁰NSC Kharkiv Institute of Physics and Technology (NSC KIPT), Kharkiv, Ukraine
⁴¹Institute for Nuclear Research of the National Academy of Sciences (KINR), Kyiv, Ukraine
⁴²University of Birmingham, Birmingham, United Kingdom
⁴³H.H. Wills Physics Laboratory, University of Bristol, Bristol, United Kingdom
⁴⁴Cavendish Laboratory, University of Cambridge, Cambridge, United Kingdom
⁴⁵Department of Physics, University of Warwick, Coventry, United Kingdom
⁴⁶STFC Rutherford Appleton Laboratory, Didcot, United Kingdom
⁴⁷School of Physics and Astronomy, University of Edinburgh, Edinburgh, United Kingdom
⁴⁸School of Physics and Astronomy, University of Glasgow, Glasgow, United Kingdom
⁴⁹Oliver Lodge Laboratory, University of Liverpool, Liverpool, United Kingdom
⁵⁰Imperial College London, London, United Kingdom
⁵¹School of Physics and Astronomy, University of Manchester, Manchester, United Kingdom
⁵²Department of Physics, University of Oxford, Oxford, United Kingdom
⁵³Syracuse University, Syracuse, NY, United States
⁵⁴Pontifícia Universidade Católica do Rio de Janeiro (PUC-Rio), Rio de Janeiro, Brazil, associated to ²
⁵⁵Institut für Physik, Universität Rostock, Rostock, Germany, associated to ¹¹

^aP.N. Lebedev Physical Institute, Russian Academy of Science (LPI RAS), Moscow, Russia

^bUniversità di Bari, Bari, Italy

^cUniversità di Bologna, Bologna, Italy

^dUniversità di Cagliari, Cagliari, Italy

^eUniversità di Ferrara, Ferrara, Italy

^fUniversità di Firenze, Firenze, Italy

^gUniversità di Urbino, Urbino, Italy

^hUniversità di Modena e Reggio Emilia, Modena, Italy

ⁱUniversità di Genova, Genova, Italy

^jUniversità di Milano Bicocca, Milano, Italy

^kUniversità di Roma Tor Vergata, Roma, Italy

^lUniversità di Roma La Sapienza, Roma, Italy

^mUniversità della Basilicata, Potenza, Italy

ⁿLIFAELS, La Salle, Universitat Ramon Llull, Barcelona, Spain

^oHanoi University of Science, Hanoi, Viet Nam

^pMassachusetts Institute of Technology, Cambridge, MA, United States

The decay $B^0 \rightarrow K^{*0}(\rightarrow K^+\pi^-)\mu^+\mu^-$ is a flavour changing neutral current process which proceeds via electroweak loop and box diagrams in the Standard Model (SM) [1]. The decay is highly suppressed in the SM and therefore physics beyond the SM such as supersymmetry [2] can contribute with a comparable amplitude via gluino or chargino loop diagrams. A number of observables are sensitive to such contributions, including the partial rate of the decay, the $\mu^+\mu^-$ forward-backward asymmetry (A_{FB}) and the CP asymmetry (\mathcal{A}_{CP}). The CP asymmetry for $B^0 \rightarrow K^{*0}\mu^+\mu^-$ is defined as

$$\mathcal{A}_{CP} = \frac{\Gamma(\bar{B}^0 \rightarrow \bar{K}^{*0}\mu^+\mu^-) - \Gamma(B^0 \rightarrow K^{*0}\mu^+\mu^-)}{\Gamma(\bar{B}^0 \rightarrow \bar{K}^{*0}\mu^+\mu^-) + \Gamma(B^0 \rightarrow K^{*0}\mu^+\mu^-)} \quad (1)$$

where Γ is the decay rate and the initial flavour of the B meson is tagged by the charge of the kaon from the K^* decay. The CP asymmetry is predicted to be of the order 10^{-3} in the SM [3, 4], but is sensitive to physics beyond the SM that changes the operator basis by modifying the mixture of the vector and axial-vector components [5, 6]. Some models that include new phenomena enhance the observed CP asymmetry up to ± 0.15 [7]. The theoretical prediction within a given model has a small error as the form factor uncertainties, which are the dominant theoretical errors for the decay rate, cancel in the ratio.

The CP asymmetry in $B^0 \rightarrow K^{*0}\mu^+\mu^-$ decays has previously been measured by the Belle [8] and BaBar [9] collaborations, with both results consistent with the SM. The LHCb collaboration has recently demonstrated its potential in this area with the most precise measurement of A_{FB} [10], and in this Letter, the measurement of the CP asymmetry by LHCb is presented.

The LHCb detector [11] is a single-arm forward spectrometer covering the pseudo-rapidity range $2 < \eta < 5$, designed for the study of particles containing b or c quarks. The detector includes a high precision tracking system consisting of a silicon-strip vertex detector surrounding the pp interaction region, a large-area silicon-strip detector located upstream of a dipole magnet with a bending power of about 4 Tm, and three stations of silicon-strip detectors and straw drift-tubes placed downstream. The combined tracking system has a momentum resolution $\Delta p/p$ that varies from 0.4% at $5\text{ GeV}/c$ to 0.6% at $100\text{ GeV}/c$, and an impact parameter (IP) resolution of $20\text{ }\mu\text{m}$ for tracks with high transverse momentum (p_T). Charged hadrons are identified using two ring-imaging Cherenkov detectors. Photon, electron and hadron candidates are identified by a calorimeter system consisting of scintillating-pad and pre-shower detectors, an electromagnetic calorimeter and a hadronic calorimeter. Muons are identified by a system composed of alternating layers of iron and multiwire proportional chambers. The trigger consists of a hardware stage, based on information from the calorimeter and muon systems, followed by a software stage which makes use of a full event reconstruction.

The simulated events used in this analysis are produced using the PYTHIA 6.4 generator [12], with a choice of parameters specifically configured for LHCb [13]. The EVTGEN package [14] describes the decay of the particles and the GEANT4 toolkit [15] simulates the detector response, implemented as described in Ref. [16]. QED radiative corrections are generated with the PHOTOS package [17].

The events used in the analysis are selected by a dedicated muon hardware trigger and then by one or more of a set of different muon and topological software triggers [18, 19]. The hardware trigger requires the muons have p_T greater than $1.48 \text{ GeV}/c$, and the software trigger requires that one of the final state particles to have both $p_T > 0.8 \text{ GeV}/c$ and IP with respect to all pp interaction vertices $> 100 \mu\text{m}$ [19]. Triggered candidates are subject to the same two-stage selection as that used in Ref. [10]. The first stage is a cut-based selection, which includes requirements on the B^0 candidate's vertex fit χ^2 , flight distance and invariant mass, and each track's impact parameters with respect to any interaction vertex, p_T and polar angle. Background from misidentified kaon and pion tracks is removed using information from the particle identification (PID) system, and muon tracks are required to have hits in the muon system. Finally, the production vertex of the B^0 candidate must lie within 5 mm of the beam axis in the transverse directions, and within 200 mm of the average interaction position in the beam (z) direction.

In the second stage, the candidates must pass a multivariate selection that uses a boosted decision tree (BDT) [20] that implements the AdaBoost algorithm [21]. This is a tighter selection which takes into account other variables including the decay time and flight direction of the B^0 candidates, the p_T of the hadrons, measures of the track and vertex quality, and PID information for the daughter tracks. For the rest of the Letter, the inclusion of charge conjugate modes is implied unless explicitly stated.

In order to obtain a clean sample of $B^0 \rightarrow K^{*0} \mu^+ \mu^-$ decays, the $c\bar{c}$ resonant decays $B^0 \rightarrow J/\psi K^{*0}$ and $B^0 \rightarrow \psi(2S)K^{*0}$ are removed by excluding events with $\mu^+ \mu^-$ invariant mass, $m_{\mu^+ \mu^-}$, satisfying $2.95 < m_{\mu^+ \mu^-} < 3.18 \text{ GeV}/c^2$ or $3.59 < m_{\mu^+ \mu^-} < 3.77 \text{ GeV}/c^2$. If $m_{K^+ \pi^- \mu^+ \mu^-} < 5.23 \text{ GeV}/c^2$, then the vetoes are extended downwards by $0.15 \text{ GeV}/c^2$ to remove the radiative tails of the resonances. Backgrounds involving misidentified particles are vetoed using cuts on the masses of the B^0 and K^{*0} mesons and the $\mu^+ \mu^-$ pair, as well as using the PID information for the daughter particles. These include $B_s^0 \rightarrow \phi \mu^+ \mu^-$ candidates in which a kaon has been misidentified as a pion, $B^0 \rightarrow J/\psi K^{*0}$ candidates where a hadron is swapped with a muon and $B^+ \rightarrow K^+ \mu^+ \mu^-$ candidates which combine with a random low momentum pion. The vetoes are described fully in Ref. [10]. \mathcal{A}_{CP} may be diluted by $B^0 \rightarrow K^{*0} \mu^+ \mu^-$ candidates with the kaon and pion misidentified as each other, which is estimated as 0.8% of the $B^0 \rightarrow K^{*0} \mu^+ \mu^-$ yield using simulated events. All B^0 candidates must have a mass in the range $5.15 - 5.80 \text{ GeV}/c^2$, the tight low mass edge of this window serves to remove background from partially reconstructed B meson decays. All K^{*0} candidates must have an invariant mass of the kaon-pion pair within $0.1 \text{ GeV}/c^2$ of the nominal $K^{*0}(892)$ mass. A proton veto, using PID information from a neural network, is also applied to remove background from Λ_b decays, where a proton in the final state is misidentified as a kaon or pion in the $B^0 \rightarrow K^{*0} \mu^+ \mu^-$ decay.

Approximately 2% of selected events contain two $B^0 \rightarrow K^{*0} \mu^+ \mu^-$ candidates which have tracks in common. The majority of these candidates arise from swapping the assignment of the kaon and pion hypothesis. As the charges of the kaon and pion tag the flavour of the B meson these duplicate candidates can bias the measured value of \mathcal{A}_{CP} . This is accounted for by randomly removing one of the two candidates from the sample. This process is repeated many times over the full sample with a different random seed in

each case and the average measured value of \mathcal{A}_{CP} is taken as the result.

An accurate measurement of \mathcal{A}_{CP} requires that the differences in the production rates (R) of B^0/\bar{B}^0 mesons and detection efficiencies (ϵ) between the $B^0 \rightarrow K^{*0}\mu^+\mu^-$ and $\bar{B}^0 \rightarrow \bar{K}^{*0}\mu^+\mu^-$ modes be accounted for. Assuming all asymmetries are small the raw measured asymmetry may be expressed as

$$\mathcal{A}_{RAW} = \mathcal{A}_{CP} + \kappa\mathcal{A}_P + \mathcal{A}_D, \quad (2)$$

where the production asymmetry, which is of the order of 1% [22], is defined as $\mathcal{A}_P \equiv [R(\bar{B}^0) - R(B^0)] / [R(\bar{B}^0) + R(B^0)]$ and the detection asymmetry is $\mathcal{A}_D \equiv [\epsilon(\bar{B}^0) - \epsilon(B^0)] / [\epsilon(\bar{B}^0) + \epsilon(B^0)]$. The production asymmetry is diluted through B^0 - \bar{B}^0 oscillations by a factor κ

$$\kappa \equiv \frac{\int_0^\infty \epsilon(t)e^{-\Gamma t} \cos \Delta m t \, dt}{\int_0^\infty \epsilon(t)e^{-\Gamma t} \, dt}, \quad (3)$$

where t , Γ , and Δm are the decay time, mean decay rate, and mass difference between the light and heavy eigenstates of the B^0 meson respectively. The quantity \mathcal{A}_D is dominated by the $K^+\pi^-/K^-\pi^+$ detection asymmetry which arises due to left-right asymmetries in the LHCb detector and different interactions of positively and negatively charged tracks with the detector material. The left-right asymmetry is cancelled by taking an average with equal weights of the CP asymmetries measured in two independent data samples with opposite polarities of the LHCb dipole magnet. These data samples correspond to 61% and 39% of the total data sample.

The production and interaction asymmetries are corrected for using the $B^0 \rightarrow J/\psi K^{*0}$ decay mode as a control channel. Since $B^0 \rightarrow K^{*0}\mu^+\mu^-$ and $B^0 \rightarrow J/\psi K^{*0}$ decays have the same final state and similar kinematics, the measured raw asymmetry for $B \rightarrow J/\psi K^{*0}$ decays may be simply expressed as $\mathcal{A}_{RAW}(B^0 \rightarrow J/\psi K^{*0}) = \kappa\mathcal{A}_P + \mathcal{A}_D$, in the absence of a CP asymmetry. $B^0 \rightarrow J/\psi K^{*0}$ proceeds via a $b \rightarrow c\bar{s}$ transition, as does the decay mode $B^+ \rightarrow J/\psi K^+$, and hence should have a CP asymmetry similar to $\mathcal{A}_{CP}(B^+ \rightarrow J/\psi K^+) = (1 \pm 7) \times 10^{-3}$ [23, 24]. For this analysis, it is assumed that $\mathcal{A}_{CP}(B^0 \rightarrow J/\psi K^{*0}) = 0$. The CP asymmetry in $B^0 \rightarrow K^{*0}\mu^+\mu^-$ decays is then calculated as

$$\mathcal{A}_{CP} = \mathcal{A}_{RAW}(B^0 \rightarrow K^{*0}\mu^+\mu^-) - \mathcal{A}_{RAW}(B^0 \rightarrow J/\psi K^{*0}). \quad (4)$$

Non-cancelling asymmetries due to differences between the kinematics of $B^0 \rightarrow K^{*0}\mu^+\mu^-$ and $B^0 \rightarrow J/\psi K^{*0}$ decays are considered as systematic effects.

The full data sample, containing approximately 900 $B^0 \rightarrow K^{*0}\mu^+\mu^-$ signal decays, is split into the six bins of $\mu^+\mu^-$ invariant mass squared (q^2) used by the LHCb, Belle, and CDF angular analyses [8, 10, 25]. An additional bin of $1 < q^2 < 6 \text{ GeV}^2/c^4$ is used, to be compared to the theoretical prediction in Ref. [4]. The $B^0 \rightarrow J/\psi K^{*0}$ data sample contains approximately 104000 signal decays with $3.04 < q^2 < 3.16 \text{ GeV}^2/c^4$. The values of \mathcal{A}_{CP} are measured using a simultaneous unbinned maximum-likelihood fit to the $B^0 \rightarrow K^{*0}\mu^+\mu^-$ and $B^0 \rightarrow J/\psi K^{*0}$ invariant mass distributions in the range $5.15 - 5.80 \text{ GeV}/c^2$. The simultaneous fit in each q^2 bin spans eight data samples, split between the initial

particles B^0 and \bar{B}^0 , the decay modes $B^0 \rightarrow K^{*0}\mu^+\mu^-$ and $B^0 \rightarrow J/\psi K^{*0}$, and magnet polarity, where the $B^0 \rightarrow J/\psi K^{*0}$ sample is common to all q^2 bins. This fit returns two values of \mathcal{A}_{CP} , one for each magnet polarity, and an average with equal weights is made to find the value of \mathcal{A}_{CP} in that q^2 bin. An integrated value of \mathcal{A}_{CP} over all q^2 is also calculated.

The signal invariant mass distributions for the $B^0 \rightarrow K^{*0}\mu^+\mu^-$ and $B^0 \rightarrow J/\psi K^{*0}$ decays are modelled using the sum of two Crystal Ball functions [26] with common peak and tail parameters but different widths. The values of the tail parameters are determined from fits to simulated events and fixed in the fit. Combinatorial background arising from the random misassociation of tracks to form a B^0 candidate is modelled using an exponential function. The $B^0 \rightarrow J/\psi K^{*0}$ fit also accounts for a peaking $B_s^0 \rightarrow J/\psi \bar{K}^{*0}$ contribution, which has the same shape as the signal and an expected yield which is $(0.7 \pm 0.2)\%$ of that of $B^0 \rightarrow J/\psi K^{*0}$ [27]. In the simultaneous fit, the signal shape is the same for the two modes, but the signal and background yields and the exponential background parameter may vary. Figure 1 shows the mass fit to the $B^0 \rightarrow K^{*0}\mu^+\mu^-$ decay in the full q^2 range.

Many sources of systematic uncertainty cancel in the difference of the raw asymmetries between $B^0 \rightarrow K^{*0}\mu^+\mu^-$ and $B^0 \rightarrow J/\psi K^{*0}$ decays and in the average of CP asymmetries measured using data recorded with opposite magnet polarities. However, systematic uncertainties can arise from residual non-cancelling asymmetries due to the different kinematic behaviour of $B^0 \rightarrow K^{*0}\mu^+\mu^-$ and $B^0 \rightarrow J/\psi K^{*0}$ decays. The effect is estimated by reweighting $B^0 \rightarrow J/\psi K^{*0}$ candidates so that their kinematic variables are distributed in the same way as for $B^0 \rightarrow K^{*0}\mu^+\mu^-$ candidates. The value of $\mathcal{A}_{RAW}(B^0 \rightarrow J/\psi K^{*0})$ is then calculated for these reweighted events and the difference from the default value is taken as the systematic uncertainty. This procedure is carried out separately for a number of quantities including the p , p_T , and pseudorapidity of the B^0 and the K^{*0} mesons. The total systematic uncertainty associated to the different kinematic behaviour of the two decays is calculated by adding each individual contribution in quadrature. This is conservative, as many of the variables are correlated.

The random removal of multiple candidates discussed above also introduces a systematic uncertainty on \mathcal{A}_{CP} . The uncertainty on the mean value of \mathcal{A}_{CP} from the ten different random removals is taken as the systematic uncertainty.

The forward-backward asymmetry in $B^0 \rightarrow K^{*0}\mu^+\mu^-$ decays [10], which varies as a function of q^2 , causes positive and negative muons to have different momentum distributions. Different detection efficiencies for positive and negative muons introduce an asymmetry that cannot be accounted for by the $B^0 \rightarrow J/\psi K^{*0}$ decay, which does not have a comparable forward-backward asymmetry. The selection efficiencies for positive and negative muons are evaluated using muons from J/ψ decay in data and the resulting asymmetry in the selected $B^0 \rightarrow K^{*0}\mu^+\mu^-$ sample is calculated in each q^2 bin.

A number of possible effects due to the choice of model for the mass fit are considered. The signal model is replaced with a sum of two Gaussian distributions and a possible difference in the mass resolution for $B^0 \rightarrow K^{*0}\mu^+\mu^-$ and $B^0 \rightarrow J/\psi K^{*0}$ decays is investigated by allowing the width of the $B^0 \rightarrow K^{*0}\mu^+\mu^-$ signal peak to vary in a range of

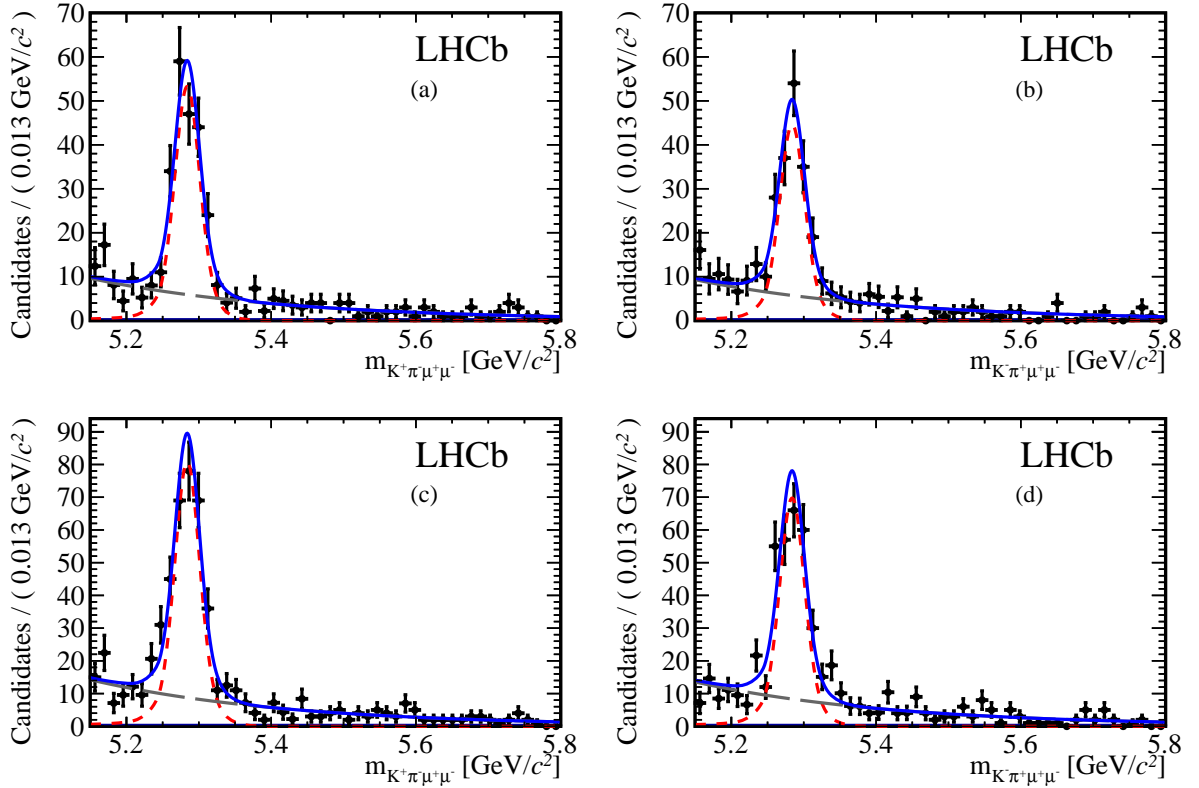


Figure 1: Mass fits for $B^0 \rightarrow K^{*0}\mu^+\mu^-$ decays used to extract the integrated CP asymmetry. The curves displayed are the full mass fit (blue, solid), the signal peak (red, short-dashed), and the background (grey, long-dashed). The mass fits on the top row correspond to the (a) B^0 and (b) \bar{B}^0 decays for one magnet polarity, while the bottom row shows the mass fits for (c) B^0 and (d) \bar{B}^0 for the reverse polarity.

0.7–1.3 times that of the $B^0 \rightarrow J/\psi K^{*0}$ model. As a further cross-check, \mathcal{A}_{CP} is calculated using a weighted average of the measurements from the six q^2 bins and the result is found to be consistent with that obtained from the integrated dataset.

The results of the full \mathcal{A}_{CP} fit are presented in Table 2 and Figure 2. The raw asymmetry in $B^0 \rightarrow J/\psi K^{*0}$ decays is measured as

$$\mathcal{A}_{\text{RAW}}(B^0 \rightarrow J/\psi K^{*0}) = -0.0110 \pm 0.0032 \pm 0.0006.$$

where the first uncertainty is statistical and the second is systematic. The CP asymmetry integrated over the full q^2 range is calculated and found to be

$$\mathcal{A}_{CP}(B^0 \rightarrow K^{*0}\mu^+\mu^-) = -0.072 \pm 0.040 \pm 0.005.$$

The result is consistent with previous measurements made by Belle [8], $\mathcal{A}_{CP}(B \rightarrow K^*l^+l^-) = -0.10 \pm 0.10 \pm 0.01$, and BaBar [9], $\mathcal{A}_{CP}(B \rightarrow K^*l^+l^-) = 0.03 \pm 0.13 \pm 0.01$. This measurement is significantly more precise than all other measurements of \mathcal{A}_{CP} in $B^0 \rightarrow K^{*0}\mu^+\mu^-$ decays to date.

Table 1: Systematic uncertainties on \mathcal{A}_{CP} , from residual kinematic asymmetries, muon asymmetry, choice of signal model, and the modelling of the mass resolution, for each q^2 bin. The total uncertainty is calculated by adding the individual uncertainties in quadrature.

q^2 region (GeV $^2/c^4$)	Sources of systematic uncertainties					Total
	multiple cands.	residual asymmetries	μ^\pm detection asymmetry	signal model	mass resol.	
0.05 < q^2 < 2.00	0.002	0.007	0.005	0.005	0.001	0.010
2.00 < q^2 < 4.30	0.006	0.007	0.006	0.007	0.010	0.016
4.30 < q^2 < 8.68	0.004	0.003	0.006	0.004	0.003	0.010
10.09 < q^2 < 12.86	0.003	0.007	0.009	0.001	0.002	0.011
14.18 < q^2 < 16.00	0.001	0.006	0.007	0.001	0.001	0.009
16.00 < q^2 < 20.00	0.003	0.005	0.003	0.003	0.009	0.012
1.00 < q^2 < 6.00	0.001	0.006	0.005	0.002	0.003	0.009
0.05 < q^2 < 20.00	0.002	0.002	0.005	0.001	0.001	0.005

Table 2: Values of \mathcal{A}_{CP} for $B^0 \rightarrow K^{*0}\mu^+\mu^-$ in the q^2 bins used in the analysis.

q^2 region (GeV $^2/c^4$)	signal yield	\mathcal{A}_{CP}	statistical uncertainty	systematic uncertainty	total uncertainty
0.05 < q^2 < 2.00	168±15	-0.196	0.094	0.010	0.095
2.00 < q^2 < 4.30	72±11	-0.098	0.153	0.016	0.154
4.30 < q^2 < 8.68	266±19	-0.021	0.073	0.010	0.075
10.09 < q^2 < 12.86	157±15	-0.054	0.097	0.011	0.098
14.18 < q^2 < 16.00	116±12	-0.201	0.104	0.009	0.104
16.00 < q^2 < 20.00	128±13	0.089	0.100	0.012	0.101
1.00 < q^2 < 6.00	194±17	-0.058	0.064	0.009	0.064
0.05 < q^2 < 20.00	904±35	-0.072	0.040	0.005	0.040

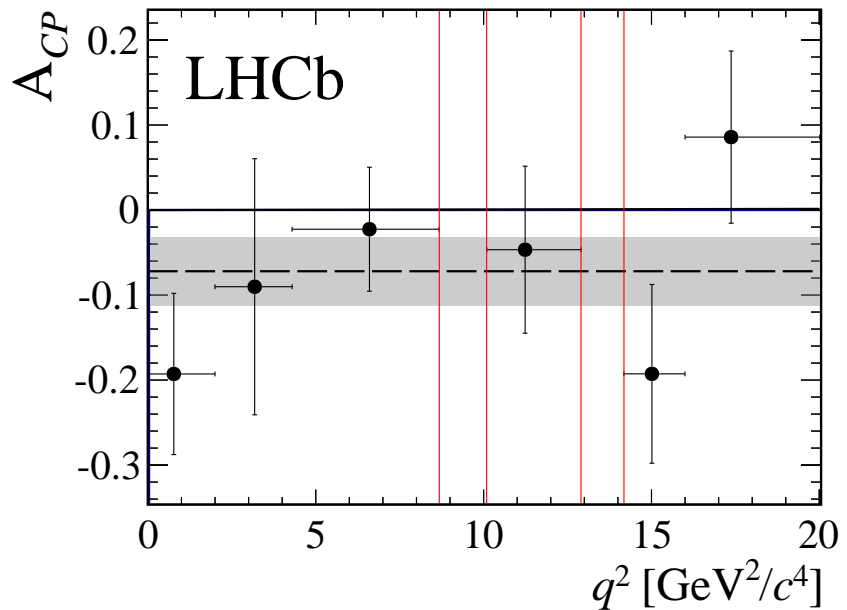


Figure 2: Fitted value of A_{CP} in $B^0 \rightarrow K^{*0}\mu^+\mu^-$ decays in bins of the $\mu^+\mu^-$ invariant mass squared (q^2). The red vertical lines mark the charmonium vetoes. The points are plotted at the mean value of q^2 in each bin. The uncertainties on each A_{CP} value are the statistical and systematic uncertainties added in quadrature. The dashed line corresponds to the q^2 integrated value, and the grey band is the 1σ uncertainty on this value.

Acknowledgements

We express our gratitude to our colleagues in the CERN accelerator departments for the excellent performance of the LHC. We thank the technical and administrative staff at the LHCb institutes. We acknowledge support from CERN and from the national agencies: CAPES, CNPq, FAPERJ and FINEP (Brazil); NSFC (China); CNRS/IN2P3 and Region Auvergne (France); BMBF, DFG, HGF and MPG (Germany); SFI (Ireland); INFN (Italy); FOM and NWO (The Netherlands); SCSR (Poland); ANCS/IFA (Romania); MinES, Rosatom, RFBR and NRC “Kurchatov Institute” (Russia); MinECo, XuntaGal and GENCAT (Spain); SNSF and SER (Switzerland); NAS Ukraine (Ukraine); STFC (United Kingdom); NSF (USA). We also acknowledge the support received from the ERC under FP7. The Tier1 computing centres are supported by IN2P3 (France), KIT and BMBF (Germany), INFN (Italy), NWO and SURF (The Netherlands), CIEMAT, IFAE and UAB (Spain), GridPP (United Kingdom). We are thankful for the computing resources put at our disposal by Yandex LLC (Russia), as well as to the communities behind the multiple open source software packages that we depend on.

References

- [1] F. Kruger, L. M. Sehgal, N. Sinha, and R. Sinha, *Angular distribution and CP asymmetries in the decays $\bar{B} \rightarrow K^-\pi^+e^-e^+$ and $\bar{B} \rightarrow \pi^-\pi^+e^-e^+$* , Phys. Rev. **D61** (2000) 114028, [arXiv:hep-ph/9907386](https://arxiv.org/abs/hep-ph/9907386).
- [2] P. Fayet and S. Ferrara, *Supersymmetry*, Phys. Rept. **32** (1977) 249.
- [3] C. Bobeth, G. Hiller, and G. Piranishvili, *CP asymmetries in bar B $\rightarrow \bar{K}^*(\rightarrow \bar{K}\pi)\ell\bar{\ell}$ and untagged \bar{B}_s , $B_s \rightarrow \phi(\rightarrow K^+K^-)\ell\bar{\ell}$ decays at NLO*, JHEP **07** (2008) 106, [arXiv:0805.2525](https://arxiv.org/abs/0805.2525).
- [4] W. Altmannshofer *et al.*, *Symmetries and asymmetries of $B \rightarrow K^*\mu^+\mu^-$ decays in the Standard Model and beyond*, JHEP **01** (2009) 019, [arXiv:0811.1214](https://arxiv.org/abs/0811.1214).
- [5] A. Ali and G. Hiller, *A theoretical reappraisal of branching ratios and CP asymmetries in the decays $B \rightarrow (X_d, X_s)\ell^+\ell^-$ and determination of the CKM parameters*, Eur. Phys. J. **C8** (1999) 619, [arXiv:hep-ph/9812267](https://arxiv.org/abs/hep-ph/9812267).
- [6] C. Bobeth, G. Hiller, D. van Dyk, and C. Wacker, *The decay $B \rightarrow Kl^+l^-$ at low hadronic recoil and model-independent $\Delta B = 1$ constraints*, JHEP **01** (2012) 107, [arXiv:1111.2558](https://arxiv.org/abs/1111.2558).
- [7] A. K. Alok *et al.*, *New physics in $b \rightarrow s\mu^+\mu^-$: CP-violating observables*, JHEP **1111** (2011) 122, [arXiv:1103.5344](https://arxiv.org/abs/1103.5344).
- [8] Belle collaboration, J.-T. Wei *et al.*, *Measurement of the differential branching fraction and forward-backward asymmetry for $B \rightarrow K^{(*)}\ell^+\ell^-$* , Phys. Rev. Lett. **103** (2009) 171801, [arXiv:0904.0770](https://arxiv.org/abs/0904.0770).

- [9] BaBar collaboration, J. Lees *et al.*, *Measurement of branching fractions and rate asymmetries in the rare decays $B \rightarrow K^{(*)}l^+l^-$* , Phys. Rev. **D86** (2012) 032012, [arXiv:1204.3933](https://arxiv.org/abs/1204.3933).
- [10] LHCb collaboration, R. Aaij *et al.*, *Differential branching fraction and angular analysis of the decay $B^0 \rightarrow K^{*0}\mu^+\mu^-$* , Phys. Rev. Lett. **108** (2012) 181806, [arXiv:1112.3515](https://arxiv.org/abs/1112.3515), LHCb-CONF-2012-008.
- [11] LHCb collaboration, A. A. Alves Jr. *et al.*, *The LHCb detector at the LHC*, JINST **3** (2008) S08005.
- [12] T. Sjöstrand, S. Mrenna, and P. Skands, *PYTHIA 6.4 physics and manual*, JHEP **05** (2006) 026, [arXiv:hep-ph/0603175](https://arxiv.org/abs/hep-ph/0603175).
- [13] I. Belyaev *et al.*, *Handling of the generation of primary events in GAUSS, the LHCb simulation framework*, Nuclear Science Symposium Conference Record (NSS/MIC) IEEE (2010) 1155.
- [14] D. J. Lange, *The EvtGen particle decay simulation package*, Nucl. Instrum. Meth. **A462** (2001) 152.
- [15] GEANT4 collaboration, J. Allison *et al.*, *Geant4 developments and applications*, IEEE Trans. Nucl. Sci. **53** (2006) 270; GEANT4 collaboration, S. Agostinelli *et al.*, *GEANT4: a simulation toolkit*, Nucl. Instrum. Meth. **A506** (2003) 250.
- [16] M. Clemencic *et al.*, *The LHCb simulation application, GAUSS: design, evolution and experience*, J. of Phys: Conf. Ser. **331** (2011) 032023.
- [17] P. Golonka and Z. Was, *PHOTOS Monte Carlo: a precision tool for QED corrections in Z and W decays*, Eur. Phys. J. **C45** (2006) 97, [arXiv:hep-ph/0506026](https://arxiv.org/abs/hep-ph/0506026).
- [18] R. Aaij and J. Albrecht, *Muon triggers in the high level trigger of LHCb*, LHCb-PUB-2011-017.
- [19] V. V. Gligorov, C. Thomas, and M. Williams, *The HLT inclusive B triggers*, LHCb-PUB-2011-016.
- [20] L. Breiman, J. H. Friedman, R. A. Olshen, and C. J. Stone, *Classification and regression trees*, Wadsworth international group, Belmont, California, USA, 1984.
- [21] R. E. Schapire and Y. Freund, *A decision-theoretic generalization of on-line learning and an application to boosting*, Jour. Comp. and Syst. Sc. **55** (1997) 119.
- [22] LHCb collaboration, R. Aaij *et al.*, *First evidence of direct CP violation in charmless two-body decays of B_s^0 mesons*, Phys. Rev. Lett. **108** (2012) 201601, [arXiv:1202.6251](https://arxiv.org/abs/1202.6251).

- [23] Particle Data Group, J. Beringer *et al.*, *Review of particle physics*, Phys. Rev. **D86** (2012) 010001.
- [24] D0 Collaboration, V. Abazov *et al.*, *Study of direct CP violation in $B^\pm \rightarrow J/\psi K^\pm(\pi^\pm)$ decays*, Phys. Rev. Lett. **100** (2008) 211802, [arXiv:0802.3299](https://arxiv.org/abs/0802.3299).
- [25] CDF collaboration, T. Aaltonen *et al.*, *Measurements of the angular distributions in the decays $B \rightarrow K^{(*)}\mu^+\mu^-$ at CDF*, Phys. Rev. Lett. **108** (2012) 081807, [arXiv:1108.0695](https://arxiv.org/abs/1108.0695).
- [26] T. Skwarnicki, *A study of the radiative cascade transitions between the Upsilon-prime and Upsilon resonances*, PhD thesis, Institute of Nuclear Physics, Krakow, 1986, DESY-F31-86-02.
- [27] LHCb collaboration, R. Aaij *et al.*, *Measurement of the $B_s^0 \rightarrow J/\psi K^{*0}$ branching fraction and angular amplitudes*, [arXiv:1208.0738](https://arxiv.org/abs/1208.0738), submitted to Phys. Rev. D (RC).